Arabian Journal of Chemistry (2020) **13**, 6341–6347

King Saud University

Arabian Journal of Chemistry

www.ksu.edu.sa
www.sciencedirect.com

ORIGINAL ARTICLE

A new technique for the synthesis of lanthanum substituted nickel cobaltite nanocomposites for the photo catalytic degradation of organic dyes in wastewater

Muhammad Ayyob [a,d], Iqbal Ahmad [c], Fiaz Hussain [b], Muhammad Kashif Bangash [b], Javeed A. Awan [a,b], Jean-Noël Jaubert [e,*]

[a] *Institute of Chemical Engineering and Technology, University of the Punjab, New Campus, 5400 Lahore, Pakistan*
[b] *Department of Textile Engineering and Technology, University of the Punjab, New Campus, 5400 Lahore, Pakistan*
[c] *Department of Chemistry, Allama Iqbal Open University, Islamabad, Pakistan*
[d] *State Key Laboratory of Fine Chemicals, School of Chemical Engineering, Dalian University of Technology, China*
[e] *Université de Lorraine, École Nationale Supérieure des Industries Chimiques, Laboratoire Réactions et Génie des Procédés (UMR CNRS 7274), 1 rue Grandville, 54000 Nancy, France*

Received 8 April 2020; accepted 29 May 2020
Available online 3 June 2020

KEYWORDS

Single step synthesis;
Metallic nanocomposites;
Wastewater treatment;
Photo catalytic activity;
Methylene blue

Abstract Developing cost-effective and more efficient nanocatalysts for the treatment of organic pollutants from process industry is always challenging for the researchers working in the field of chemistry, chemical, energy and environment engineering. In this work, a cost-effective and more efficient nanocatalysts, *i.e.*, Nickel Cobaltite nanocomposites and its Lanthanum (La) doped derivatives with controlled surface morphology has been synthesized at 393.15 K through single step sol–gel method. The surface morphology, chemical composition, and crystal structure of the synthesized nanocomposites were analysed by scanning electron microscopy (SEM), Fourier transformed infrared spectroscopy (FTIR), and X-rays diffraction (XRD), respectively. The rough surface and well-crystallized metallic nanocomposites confirm the successful synthesis of nanocatalysts. The molar ratio of Lanthanum to Cobalt (La_x:Co_y) showed a significant influence on the surface morphology and catalytic activity (K_{app} = 0.15–0.47 min^{-1}) of the products. Synthesized nanocomposites showed high catalytic activity for the reduction of methylene blue under solar irradiation. Photo-

* Corresponding author.
E-mail address: jean-noel.jaubert@univ-lorraine.fr (J.-N. Jaubert).
Peer review under responsibility of King Saud University.

Production and hosting by Elsevier

https://doi.org/10.1016/j.arabjc.2020.05.036

catalytic results for the reduction of methylene blue show that the catalytic activity of synthesized nanocatalysts increases with the increase in the doping concentration of Lanthanum.

1. Introduction

With growing concerns about organic pollutants and water pollution, it becomes important to find suitable catalysts for wastewater treatment in industrial processes. Metallic nanocatalysts have been widely developed and synthesized for their potential applications in the fields of catalysis (Hussain et al., 2019), plasmonics (Trendafilov et al., 2019), biosensors and medicine (Majdalawieh et al., 2014). Among the various metallic nanomaterials, Nickel (Ni) and Cobalt (Co) based nanomaterials are of special interest due to their exceptional performance, low cost, low toxicity, natural abundance, and morphologies. Several researchers have attempted the synthesis of Ni-Co nanoparticles and reported their potential applications in the fields of supercapacitors (Tseng et al., 2013), electrochemistry (Chen et al., 2014) and biosensors (Deepalakshmi et al., 2018). However, the development of Ni-Co based metallic nanocomposites and their application for treatment of organic pollutants has not been well explored yet.

Nanoparticles have exceptional degradation behaviour due to their nano size and large surface area which enable them to be attached on the surface of any supporting material for the reduction of toxic organic pollutants. Methylene blue (MB) is a very toxic dye which may cause serious health problems such as severe headache, fever, hypertension, allergy, mental disorder, stomach and bladder irritations (Ramsay et al., 2007; Harvey and Keitt, 1983; Mokhlesi et al., 2003). Therefore, the treatment of such hazardous dyes is very important. One of the most effective techniques for the treatment of chronic organic dyes is their photocatalytic degradation in the presence of nanocatalysts, because they are reusable and recyclable photocatalysts (Yola et al., 2014).

Metal nitrides have been recognized as new advance materials with exceptional electrical conductivity, catalytic reactivity, mechanical strength and interstitial alloy behaviour (Li et al., 2017). Among other metal nitrides, Cobalt nitride has attracted significant attention due to its superior electrical conductivity, chemical resistance and corrosion resistance (Zhang et al., 2016). The ternary metal nitrides like $NiLa_xCo_yO_4$ have higher redox kinetics compared to binary metal nitrides and execute superior catalytic and electrochemical properties (Wang et al., 2016; Sun et al., 2015; Yuan et al., 2017). Therefore, the synthesis of nanocomposites of Ni, La, and Co ($NiLa_xCo_yO_4$) has been carried out and their catalytic activity has been successfully tested for the reduction of methylene blue. It is worthy to note that compared to conventional methods used for the synthesis of ternary metal nitrides, which are generally complex, multi-step and that require high energy input, the adopted sol–gel method is facile, single-step and requires low energy input. Due to high production efficiency and ease of production this method can easily be extended to an industrial scale.

In this work, a facile, low cost, scalable and single-step one-pot approach to develop a series of $NiLa_xCo_yO_4$ nanocomposites catalyst through a sol–gel method is adopted. The synthesized nanocomposites are characterized by their morphology and catalytic behaviour. The effects of La addition and change in molar ratio of La and Co (La_x:Co_y) in the $NiLa_xCo_yO_4$ nanocomposites has been studied. The synthesized $NiLa_xCo_yO_4$ nanocomposites showed excellent photocatalytic activity towards the reduction of MB. To the best of authors knowledge, it is the first time that such an efficient catalyst based on Ni, La and Co metal nitrides is being reported for the reduction of an organic pollutant like MB.

2. Materials and methods

2.1. Materials

Nickel nitrate ($Ni(NO_3)_2{\cdot}6H_2O$, 99.9% purity), cobalt nitrate ($Co(NO_3)_2{\cdot}6H_2O$, 99.0% purity), and lanthanum nitrate ($La(NO_3)_2{\cdot}6H_2O$, 99.9% purity) were purchased from Merck, Germany. The citric acid ($C_6H_8O_7$, 99.5% purity) and ammonia solution (NH_3, 33% purity) were purchased from BDH chemicals, Pakistan. All the analytical grade chemicals were used as received without any further purification. Ultra-pure deionized (DI) water and freshly prepared solutions were used during the experiments.

2.2. Synthesis of Nickel lanthanum-cobalt ($NiLa_xCo_yO4$) metallic nanocomposites

Ni, La and Co nanocomposites were prepared by the sol–gel method. Fresh solutions of Nickel nitrate (0.1 M), Cobalt nitrate (0.2 M), Lanthanum nitrate (0.2 M) and citric acid (0.3 M) were prepared in DI water. A homogeneous mixture of all the chemicals was placed on the hot stirrer plate and heated up to 393.15 K while stirring at 250 RPM. Ammonia solution (2.0 M) was added dropwise for adjusting pH of the solution to 7.0 and the reaction conditions were maintained for 3 h. After the completion of the reaction, the synthesized product was purified by washing with water and it was placed in the vacuum oven for two hours at 50 °C and sintered at 400 °C for two hours in a muffle furnace. The amount of Ni specie remained same in all the samples. Four samples with different concentration of La substitution (La_x:Co_y) (0.00: 2.0, 0.05; 1.95, 0.1: 1.90, 0.15: 1.85 M) were prepared by following the same protocol reported above.

2.3. Characterization

The surface morphology of the synthesized $NiLa_xCo_yO_4$ nanocomposites was analysed by scanning electron microscope (SEM, HITACHI SU800) at an accelerating voltage of 15 kV.

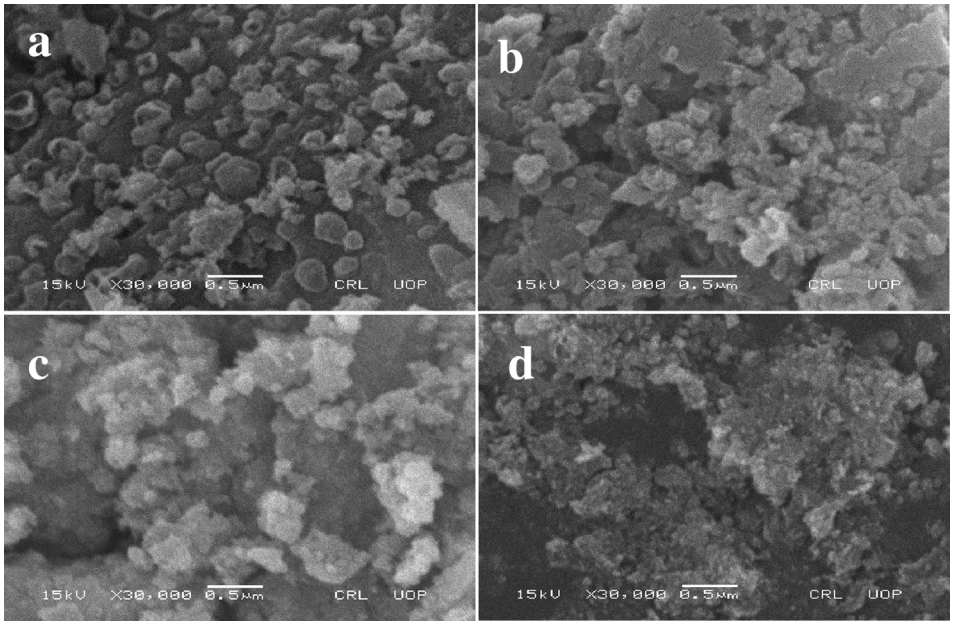

Fig. 1 FE-SEM micrographs of synthesized $NiLa_xCo_yO_4$ nanocomposites (a) $NiLa_{0.0}Co_2O_4$ (b) $NiLa_{o.o5}Co_{1.95}O_4$ (c) $NiLa_{o.1}Co_{1.9}O_4$ and (d) $NiLa_{o.15}Co_{1.85}O_4$ nanocomposites.

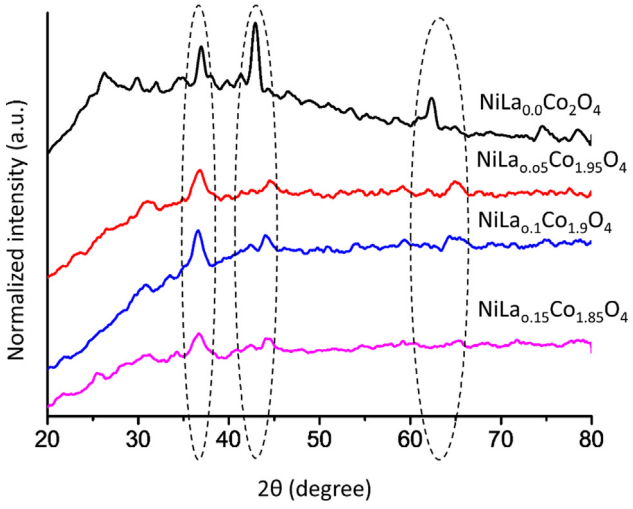

Fig. 2 XRD patterns of $NiLa_xCo_yO_4$ (x = 0.0–0.15) nanoparticles.

The phase formation, purity, and crystalline features of the nanocomposites were determined by a powder X-ray Diffraction (XRD, Rigaku Smartlab) using Cu Kα radiation (λ = 1.54060 Å) operating at 40 kV. The samples were scanned in the 2θ range of 20-80° with a scanning speed of 2θ/min. The chemical composition of the synthesized $NiLa_x$-Co_yO_4 nanocomposites was analysed by the Fourier transform infrared spectrometer (FTIR, Nicolet iS50 110 V/lnGaAs). The powder samples for FTIR were dried in the oven at 50 °C for two hours. The samples were scanned in the range of 300–4000 cm^{-1} with a scanning speed of 4 mm/min.

2.4. Photocatalytic reduction activity of $NiLa_xCo_yO_4$ nanocomposites

The photocatalytic activity was determined against an industrial dye, methylene blue. In a typical procedure, a light source (450 W, Xe arc lamp) operated at 200 W was used for the photocatalytic degradation. The Light was passed through two filters, 10 cm IR filter and cut off filter (λ > 300 nm), and it was focused to the reaction mixture. The reaction mixture, 10 mL of freshly prepared MB solution ($1x10^{-4}$ M) mixed with 1 mg of synthesized $NiLa_xCo_yO_4$ nanocatalysts was loaded into the Pyrex glass cell. 5 mL of the mixture was taken, and UV–Vis spectroscopy was performed at different intervals of time (min) in the range of 500–800 nm.

3. Results and discussion

3.1. Characterization of $NiLa_xCo_yO_4$ nanocomposites

The morphology of the synthesized $NiLa_xCo_yO_4$ nanocomposites was examined using FE-SEM. Fig. 1(a) shows the surface morphology of pure Nickel Cobalt nanocomposites ($NiLa_{0.0}$-$Co_{2.0}O_4$) and Fig. 1(b), 1(c) and 1(d) show the La-doped Nickel Cobalt nanocomposites. The pictures highlight that (i) all the samples have different surface morphology and (ii) surface roughness increases with increasing the doping concertation of La in the synthesized $NiLa_xCo_yO_4$ nanocomposites.

The phase composition and crystalline structure of the synthesized nanocomposites were analyzed using XRD. Fig. 2 shows that all the samples exhibited similar diffraction peaks, that matches with the standard diffraction data (PDF. No. 73-1702) (Guan et al., 2019). XRD pattern showed characteristics diffraction peaks at 35.5°; 43°, and 63° that corresponds to

(3 1 1), (4 0 0) and (4 4 0) planes of face catered cubic (FCC) structure, respectively. The crystallite size of $NiLa_xCo_yO_4$ nanocomposites was calculated using the Debye–Scherrer equation and found to be ~15 nm. Such results confirm the formation of pure and well crystallized $NiLa_xCo_yO_4$ nanocomposites. It is also clear from the results that the intensity of the characteristic diffraction peaks decreases with increasing the doping concentrations of La. This behaviour can be due to appearance of new amorphous regions by increasing the doping concertation of La. It is important to note that analysed XRD results are in accordance to FE-SEM results.

The chemical composition of the synthesized $NiLa_xCo_yO_4$ nanocomposites was analysed using FTIR and the results are shown in Fig. 3. They confirm the successful modification of Nickel Cobaltite nanocomposites with La. For the sample (a) ($NiLa_{0.0}Co_{2.0}O_4$), the band at 3,270 cm^{-1} is attributed to the –OH stretching of the molecular water and of hydrogen-bond O–H group, and the sharp absorbance bands at 2,251 can be assigned to CH– symmetric stretching. The clear signal at 1,360 cm^{-1} is due to the symmetric vibrations of COO–. The peak at 1,098 cm^{-1} is attributed to the C–O stretching and confirms the presence of C–O in the ($NiLa_{0.0}Co_{2.0}O_4$). The absorbance band at 804 cm^{-1} can be attributed to the –CH2 twisting and C–COOH stretching. It is noteworthy that all the characteristic peaks observed in $NiLa_{0.0}Co_{2.0}O_4$ nanocomposites were also observed in all other samples that were doped with different concentrations of La. The different small peaks appearing between around 710, 850, and 1070 cm^{-1} are due to the stretching vibration of C–O in the $NiLa_xCo_yO_4$ nanocomposites. It is important to note that FTIR results agree well with previously reported findings (Zahariev et al., 2017; Markova-Deneva, 2010) thereby confirming that $NiLa_xCo_yO_4$ nanocomposites were successfully synthesized.

3.2. Photolysis of MB

As a control experiment, photolysis was performed to compare with the adsorption and photocatalytic results. Dark reaction was performed in the absence of UV and catalyst while photolysis was performed with UV (in the absence of catalyst). Dark reaction and photolysis were compared, and the results are present in Fig. 4. It is evident from the results that about 94% MB is not degraded even after 1 h in dark condition. It was also found that the MB could be degraded in the absence of catalyst under UV irradiation but only very slowly because even after 1 h, only 21% is degraded. El-Sharkawy et al. (El-Sharkawy et al., 2007) observed that in the absence of catalyst about 37% of MB do not degrade when irradiated with UV even after 1500 min.

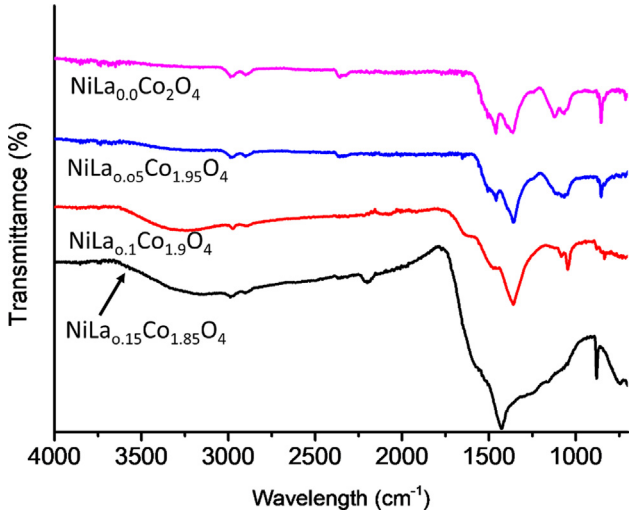

Fig. 3 FTIR spectrum of synthesized $NiLa_xCo_yO_4$ nanoparticles.

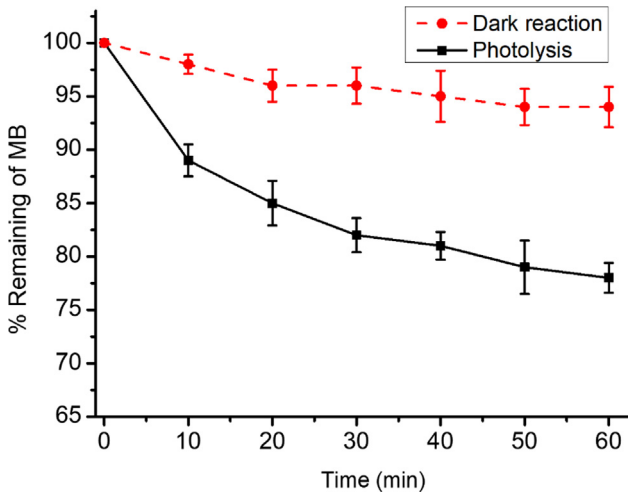

Fig. 4 Dark reaction and photolysis of MB (12 mg/L).

3.3. Catalytic reduction of MB

The catalytic performance of the synthesized $NiLa_xCo_yO_4$ nanocatalysts was analysed in terms of the reduction of methylene blue (MB) to leuco-methylene blue (LMB). The catalytic behaviour was evaluated by UV–Vis spectroscopy at different time intervals and catalyst type. In the absence of the synthesized $NiLa_xCo_yO_4$ catalysts, the characteristic absorption peak of MB at λ = 664 nm does not decrease even after 24 h. As can be concluded from Fig. 5, under the same conditions, the addition of prepared nanocatalysts results in the gradual decrease in the absorption peak of MB at λ = 664 nm with an obvious change in the blue colour of MB, indicating the reduction of MB into LMB. The intensity of the absorption peak continues to decrease until the complete reduction of the MB. Depending on the type of nanocatalyst sample, complete reduction is reached at different times.

The reaction rate constant (k_{app}) for the reduction of the organic pollutant (MB in this study) was determined by using Eq. (1).

$$\ln(C_t/C_o) = -k_{app}t \quad (1)$$

where C_o shows the initial concentration of the pollutant and C_t shows the concentration at a certain time t. According to the Beer-Lambert law, the ratio of C_t/C_o can be directly obtained from the corresponding absorbance A_t/A_o. So, Eq. (1) can be reconsidered as follow:

$$\ln(C_t/C_o) = \ln(A_t/A_o) = -k_{app}t \quad (2)$$

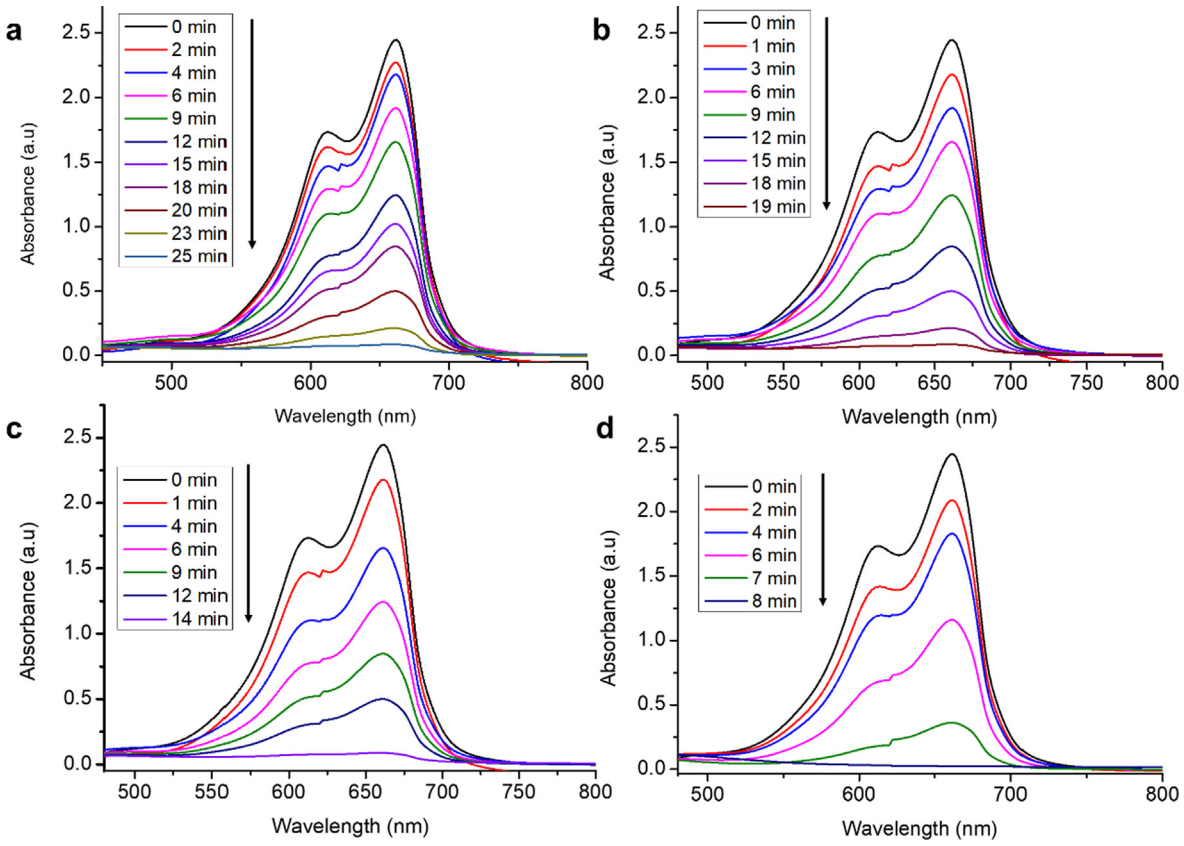

Fig. 5 Absorption spectra for the photodegradation of MB in the presence of synthesized $NiLa_xCo_yO_4$ nanocomposites (a) $NiLa_{0.0}Co_2O_4$ (b) $NiLa_{o.o5}Co_{1.95}O_4$ (c) $NiLa_{o.1}Co_{1.9}O_4$ and (d) $NiLa_{o.15}Co_{1.85}O_4$ nanocomposites.

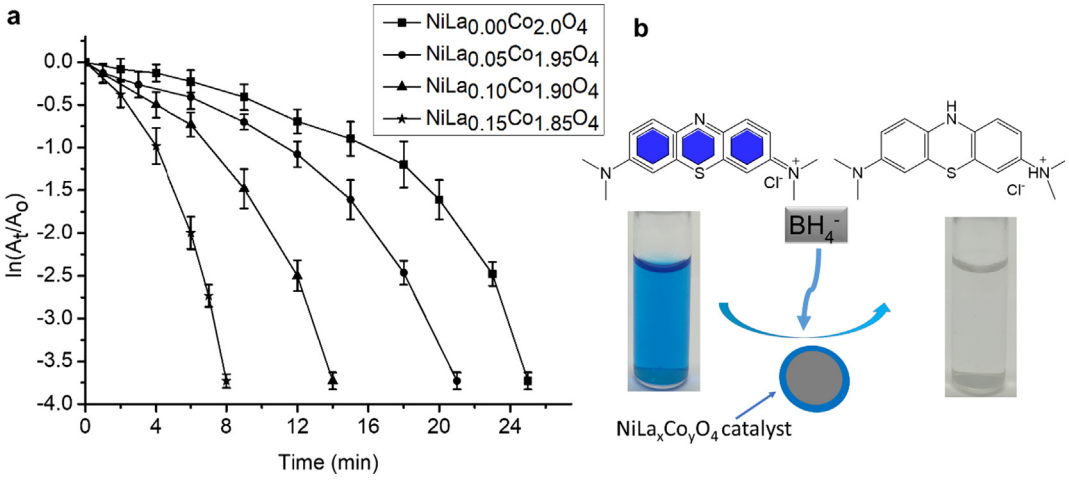

Fig. 6 (a) Plot of $\ln(A_t/A_o)$versus time for the reduction of MB into LMD in the presence of synthesized $NiLa_xCo_yO_4$ nanocomposites (error bars represent the standard deviation of four replicates); (b) Schematic diagram for the photocatalytic reduction of MB into LMB.

According to Eq. (2), k_{app} corresponds to the slope from the linear relationship between t and C_t/C_o.

The effect of the different catalysts on the reduction kinetics of MB was determined by measuring their catalytic behaviours. The reaction rates of all the nanocatalysts were determined and compared. As highlighted by Fig. 6, it was found that the reaction rate of synthesized $NiLa_xCo_yO_4$ nanocomposites increases with increasing the doping concentration of La. The rate constant of $NiLa_{o.15}Co_{1.85}O_4$ nanocatalyst; containing the highest concentration of La (0.15 M) was 320% (Kapp = 0.47 min^{-1}) higher than $NiLa_{0.0}Co_2O_4$ (Kapp = 0.15/min^{-1}) nanocatalyst; containing the lowest con-

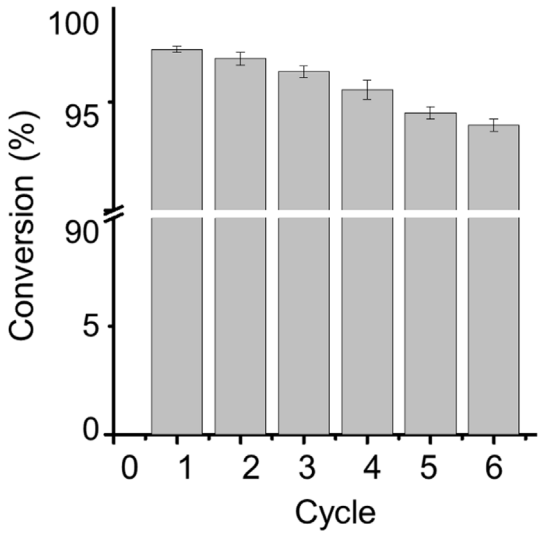

Fig. 7 Catalytic efficiency of synthesized nanocomposites after repeated uses (error bars represent the standard deviation of four replicates).

centration of La (0.00 M). The improved catalytic behaviour can be attributed to the rough surface of the nanocomposites which increases with increasing the concentration of La. Rough surface facilitates the catalytic process by providing more catalytic sites for the reduction of MB. It is believed that reactive oxygen species are generated during the catalytic process and they reduce MB. Similar findings were also reported in the open literature by P. Shao and co-workers (Shao et al., 2019; Shao et al., 2017; Shao et al., 2018).

3.4. Stability of the nanocomposites

Synthesized $NiLa_xCo_yO_4$ nanocomposites used for the degradation of MB were found to be recyclable. As an example, the $NiLa_{0.15}Co_{1.85}O_4$ catalyst was recovered from the solution after the reduction process by centrifugation. The catalytic efficiency was determined after repeated uses for up to 6 cycles and it was found to be stable with a conversion efficiency of about 98% (see Fig. 7). This recyclability indicates the colloidal stability of the synthesized nanocomposites. Furthermore, a quantitative analysis aimed at determining the possible leaching of La/Ni/Co after the repeated uses highlighted that no significant amount of La/Ni/Co was detected. Hence, it can be concluded that synthesized $NiLa_xCo_yO_4$ nanocomposites remain stable even after six successive uses.

4. Conclusion

The sol–gel method, employed for the synthesis of $NiLa_xCo_yO_4$ nanocomposites is very efficient (90.1%), facile, simple, and low-cost. The synthesized crystallized and pure $NiLa_xCo_yO_4$ nanocomposites were analysed for their surface morphology, purity, chemical composition, and crystalline nature. The morphology of the synthesized nanocomposites can be tuned by adjusting the doping concentration of La (La_x:Co_y). The prepared nanocomposites showed an efficient photocatalytic activity against the organic pollutant and displayed prominent reduction of MB at room temperature without the assistance of any other toxic chemicals. It can be concluded that developed nanocomposites can be a potential candidate for applications in areas, such as process wastewater treatment, biosensors, catalysis, electrochemical, and supercapacitors. This synthesis approach will be further extended for the synthesis of ternary metallic nanocomposites that may broaden its area of applications.

References

Chen, H., Hu, L., Chen, M., Yan, Y., Wu, L., 2014. Nickel-cobalt layered double hydroxide nanosheets for high-performance supercapacitor electrode materials. Adv. Funct. Mater. 24 (7), 934–942. https://doi.org/10.1002/adfm.201301747.

Deepalakshmi, T., Tran, D.T., Kim, N.H., Chong, K.T., Lee, J.H., 2018. Nitrogen-doped draphene-encapsulated nickel cobalt nitride as a highly sensitive and selective electrode for glucose and hydrogen peroxide sensing applications. ACS Appl. Mater. Interfaces 10 (42), 35847–35858. https://doi.org/10.1021/acsami.8b15069.

El-Sharkawy, E.A., Soliman, A.Y., Al-Amer, K.M., 2007. Comparative study for the removal of methylene blue via adsorption and photocatalytic degradation. J. Colloid Interface Sci. 310 (2), 498–508. https://doi.org/10.1016/j.jcis.2007.02.013.

Guan, X., Luo, P., Yu, Y., Li, X., Chen, D., 2019. Solvent-tuned synthesis of mesoporous nickel cobaltite nanostructures and their catalytic properties. Appl. Sci. Switz. 9, (6). https://doi.org/10.3390/app9061100.

Harvey, J.W., Keitt, A.S., 1983. Studies of the efficacy and potential hazards of methylene blue therapy in aniline-induced methaemoglobinaemia. Br. J. Haematol. 54 (1), 29–41. https://doi.org/10.1111/j.1365-2141.1983.tb02064.x.

Hussain, F., Shaban, S.M., Kim, J., Kim, D.-H., 2019. One-pot synthesis of highly stable and concentrated silver nanoparticles with enhanced catalytic activity. Korean J. Chem. Eng. 36 (6), 988–995. https://doi.org/10.1007/s11814-019-0270-6.

Li, Y.Z., Li, T.T., Chen, W., Song, Y.Y., 2017. Co4N nanowires: noble-metal-free peroxidase mimetic with excellent salt- and temperature-resistant abilities. ACS Appl. Mater. Interfaces 9 (35), 29881–29888. https://doi.org/10.1021/acsami.7b09861.

Majdalawieh, A., Kanan, M.C., El-Kadri, O., Kanan, S.M., 2014. Recent advances in gold and silver nanoparticles: synthesis and applications. J. Nanosci. Nanotechnol. 14 (7), 4757–4780. https://doi.org/10.1166/jnn.2014.9526.

Markova-Deneva, I., 2010. Infrared spectroscopy investigation of metallic nanoparticles based on copper, cobalt, and nickel synthesized through borohydrate reduction method. J. Univ. Chem. Technol. Met. 45 (4), 351–378.

Mokhlesi, B., Leikin, J.B., Murray, P., Corbridge, T.C., 2003. Adult toxicology in critical care Part II: Specific poisonings. Chest 123 (3), 897–922. https://doi.org/10.1378/chest.123.3.897.

Ramsay, R.R., Dunford, C., Gillman, P.K., 2007. Methylene blue and serotonin toxicity: inhibition of monoamine oxidase A (MAO A) confirms a theoretical prediction. Br. J. Pharmacol. 152 (6), 946–951. https://doi.org/10.1038/sj.bjp.0707430.

Shao, P., Duan, X., Xu, J., Tian, J., Shi, W., Gao, S., Xu, M., Cui, F., Wang, S., 2017. Heterogeneous activation of peroxymonosulfate by amorphous boron for degradation of bisphenol S. J. Hazard. Mater. 322, 532–539. https://doi.org/10.1016/j.jhazmat.2016.10.020.

Shao, P., Tian, J., Yang, F., Duan, X., Gao, S., Shi, W., Luo, X., Cui, F., Luo, S., Wang, S., 2018. Identification and regulation of active sites on nanodiamonds: establishing a highly efficient catalytic system for oxidation of organic contaminants. Adv. Funct. Mater. 28 (13), 1705295. https://doi.org/10.1002/adfm.201705295.

Shao, P., Tian, J., Duan, X., Yang, Y., Shi, W., Luo, X., Cui, F., Luo, S., Wang, S., 2019. Cobalt silicate hydroxide nanosheets in hierarchical hollow architecture with maximized cobalt active site for catalytic oxidation. Chem. Eng. J. 359, 79–87. https://doi.org/10.1016/j.cej.2018.11.121.

Sun, T., Wu, Q., Che, R., Bu, Y., Jiang, Y., Li, Y., Yang, L., Wang, X., Hu, Z., 2015. Alloyed Co–Mo nitride as high-performance electrocatalyst for oxygen reduction in acidic medium. ACS Catal. 5 (3), 1857–1862. https://doi.org/10.1021/cs502029h.

Trendafilov, S., Allen, M., Allen, J., Lin, Z., 2019. Comparison of octahedral and spherical nanoparticles for plasmonics. IEEE Photonics J. 11 (3), 1–6. https://doi.org/10.1109/JPHOT.2019.2919226.

Tseng, C.C., Lee, J.L., Liu, Y.M., Ger, M. Der, Shu, Y.Y., 2013. Microwave-assisted hydrothermal synthesis of spinel nickel cobaltite and application for supercapacitors. J. Taiwan Inst. Chem. Eng. 2013, 44 (3), 415–419. https://doi.org/10.1016/j.jtice.2012.12.014.

Wang, Y., Liu, D., Liu, Z., Xie, C., Huo, J., Wang, S., 2016. Porous cobalt-iron nitride nanowires as excellent bifunctional electrocatalysts for overall water splitting. Chem. Commun. 52 (85), 12614–12617. https://doi.org/10.1039/C6CC06608A.

Yola, M.L., Eren, T., Atar, N., 2014. A novel efficient photocatalyst based on TiO2 nanoparticles involved boron enrichment waste for photocatalytic degradation of atrazine. Chem. Eng. J. 250, 288–294. https://doi.org/10.1016/j.cej.2014.03.116.

Yuan, Y., Yang, L., He, B., Pervaiz, E., Shao, Z., Yang, M., 2017. Cobalt-zinc nitride on nitrogen doped carbon black nanohybrids as a non-noble metal electrocatalyst for oxygen reduction reaction. Nanoscale 9 (19), 6259–6263. https://doi.org/10.1039/C7NR02264F.

Zahariev, I., Piskin, M., Karaduman, E., Ivanova, D., Markova, I., Fachikov, L., 2017. Ftir spectroscopy method for investigation of Co-Ni nanoparticle nanosurface phenomena. J. Chem. Technol. Metall. 52 (5), 916–928.

Zhang, Y., Ouyang, B., Xu, J., Jia, G., Chen, S., Rawat, R.S., Fan, H. J., 2016. Rapid synthesis of cobalt nitride nanowires: highly efficient and low-cost catalysts for oxygen evolution. Angew. Chem. - Int. Ed. 55 (30), 8670–8674. https://doi.org/10.1002/anie.201604372.